Resting state functional atlas and cerebral networks in mouse lemur primates at 11.7 Tesla

Clément M Garin, Nachiket A Nadkarni, Brigitte Landeau, Gaël Chételat, Jean-Luc Picq, Salma Bougacha, Marc Dhenain

NeuroImage 226 (2021) 117589

Contents lists available at ScienceDirect

NeuroImage

journal homepage: www.elsevier.com/locate/neuroimage

Resting state functional atlas and cerebral networks in mouse lemur primates at 11.7 Tesla

Clément M. Garin[a,b], Nachiket A. Nadkarni[a,b], Brigitte Landeau[c,d], Gaël Chételat[c,d], Jean-Luc Picq[a,b,e], Salma Bougacha[a,b,c,d], Marc Dhenain[a,b,*]

[a] Centre National de la Recherche Scientifique (CNRS), Université Paris-Saclay, UMR 9199, Neurodegenerative Diseases Laboratory, 18 Route du Panorama, F-92265 Fontenay-aux-Roses, France
[b] Commissariat à l'Energie Atomique et aux Energies Alternatives (CEA), Direction de la Recherche Fondamentale (DRF), Institut François Jacob, MIRCen, 18 Route du Panorama, F-92265 Fontenay-aux-Roses, France
[c] Inserm, Inserm UMR-S U1237, Normandie University, UNICAEN, GIP Cyceron, Caen, France
[d] UNICAEN, EPHE, INSERM, U1077, CHU de Caen, Neuropsychologie et Imagerie de la Mémoire Humaine, Normandie University, 14000 Caen, France
[e] Laboratoire de Psychopathologie et de Neuropsychologie, EA 2027, Université Paris 8, 2 Rue de la Liberté, 93000 St Denis, France

ARTICLE INFO

Keywords:
Brain function
Cerebral networks
Functional MRI
Hubs
Microcebus murinus
Mouse lemur atlas
Resting state

ABSTRACT

Measures of resting-state functional connectivity allow the description of neuronal networks in humans and provide a window on brain function in normal and pathological conditions. Characterizing neuronal networks in animals is complementary to studies in humans to understand how evolution has modelled network architecture. The mouse lemur (*Microcebus murinus*) is one of the smallest and more phylogenetically distant primates as compared to humans. Characterizing the functional organization of its brain is critical for scientists studying this primate as well as to add a link for comparative animal studies. Here, we created the first functional atlas of mouse lemur brain and describe for the first time its cerebral networks. They were classified as two primary cortical networks (somato-motor and visual), two high-level cortical networks (fronto-parietal and fronto-temporal) and two limbic networks (sensory-limbic and evaluative-limbic). Comparison of mouse lemur and human networks revealed similarities between mouse lemur high-level cortical networks and human networks as the dorsal attentional (DAN), executive control (ECN), and default-mode networks (DMN). These networks were however not homologous, possibly reflecting differential organization of high-level networks. Finally, cerebral hubs were evaluated. They were grouped along an antero-posterior axis in lemurs while they were split into parietal and frontal clusters in humans.

1. Introduction

Different brain regions are interacting continuously to share information through functional cerebral networks built from structural and functional connections. In addition to the myriad of articles that described very precisely these networks in humans in normal and pathological conditions, many studies have evaluated cerebral networks in macaques as well as marmosets. They suggested homologies of several networks as for example the executive (Hutchison et al., 2012) or the default-mode network (DMN) (Vincent et al., 2007). Some discrepancies have however been reported. For example, the main frontal region involved in the default-mode-like network (DMN-like) of marmosets or macaques is the dorso-lateral frontal cortex (dlFC) and not the medial frontal cortex (mFC) as in the human DMN (Liu et al., 2019; Mantini et al., 2011).

To better understand the diversity of cerebral network architecture in primates, it is necessary to describe networks in primates distant from usually studied monkeys. The mouse lemur (*Microcebus murinus*) is a small strepsirrhine, arboreal and nocturnal primate (12 cm length, 60–120 g weight). It has a key position on phylogenetic trees of primates as it presents with one of the longest genetic distances with humans (Ezran et al., 2017). It is the primate with the smallest brain (1.8 g versus ~1500 g for humans (Herculano-Houzel et al., 2015)) and has a smooth brain as all animals with light brains (Mota and Herculano-Houzel, 2015) except for the sylvian and calcarine fissures. It has a small white matter/cerebrum index (Nadkarni et al., 2019) but its cerebrotype (cortex/cerebrum index) does not differ from those of other primates (Nadkarni et al., 2019). The aim of this study was to provide the first characterization of neuronal networks in mouse lemurs. Several meth-

* Corresponding author at: Centre National de la Recherche Scientifique (CNRS), Université Paris-Saclay UMR 9199, Neurodegenerative Diseases Laboratory, 18 Route du Panorama, F-92265 Fontenay-aux-Roses, France
E-mail addresses: garincle@gmail.com (C.M. Garin), nadkarni@fastmail.fm (N.A. Nadkarni), landeau@cyceron.fr (B. Landeau), chetelat@cyceron.fr (G. Chételat), jean_lucpicq@hotmail.com (J.-L. Picq), salmabougacha@hotmail.com (S. Bougacha), Marc.Dhenain@cea.fr (M. Dhenain).

https://doi.org/10.1016/j.neuroimage.2020.117589
Received 16 September 2020; Received in revised form 13 November 2020; Accepted 19 November 2020
Available online 26 November 2020

Table 1
Cohort of mouse lemurs involved in the study.

	Sex	Age (months)	Age (years)	Anatomical brain lesion
283EA	M	10.6	0.9	No
365A	M	10.6	0.9	No
285AB	M	10.7	0.9	No
285AAA	M	16.5	1.4	No
283CCA	M	16.6	1.4	No
263BCE	M	17.8	1.5	No
314CA	M	18.0	1.5	No
283CA	M	22.4	1.9	No
285E	M	22.6	1.9	No
276BC	M	28.0	2.3	No
285D	M	28.1	2.3	No
289BB	F	28.8	2.4	No
300BA	M	29.8	2.5	No
288BC	F	37.3	3.1	Yes
208CBF	F	37.5	3.1	No
310C	F	39.9	3.3	Yes

ods have been proposed to characterize brain networks (Bassett and Sporns, 2017). Amongst them, blood-oxygen level dependent (BOLD) resting-state functional magnetic resonance imaging (rsfMRI) relies on the fact that, in the absence of explicit tasks (*i.e.* in resting state conditions), patterns of oscillations of the fMRI signal are similar in functionally connected brain structures (Biswal et al., 1995). The detection of the synchronicity of BOLD signal in various brain regions in resting state conditions can thus be used to describe cerebral organization, including both local functional regions and large scale networks composed of widespread functional regions (Biswal et al., 1995; Power et al., 2014). Here, rsfMR images were recorded from 14 mouse lemurs at 11.7 Tesla. Using dictionary learning and a large number of components, we defined functional regions that were concatenated into a functional atlas of mouse lemur brains. Then, using dictionary learning and a smaller number of components, we identified 6 regional networks in mouse lemurs. The method used to identify regional networks in lemurs was applied to a dataset from 42 humans. It identified typical networks usually reported in the literature. Comparison of cerebral networks in mouse lemurs and humans revealed homologous networks as well as similar but non-homologous high-level cortical networks. Hubness evaluation revealed that hubs follow an antero-posterior axis in lemurs while they are split into parietal and frontal clusters in humans.

2. Materials and methods

2.1. Animals and breeding

This study was carried out in accordance with the recommendations of the European Communities Council directive (2010/63/EU). The protocol was approved by the local ethics committees CEtEA-CEA DSV IdF (authorization 201506051736524 VI (APAFIS#778)). All mouse lemurs studied were born in the laboratory breeding colony of CNRS/MNHN in Brunoy, France (UMR 7179 CNRS/MNHN) and bred in the Molecular Imaging Research Center (CEA, Fontenay-aux-Roses). The animals were transported from the CNRS/MNHN to the Molecular Imaging Research Center at least two months before the MRI exams.

Sixteen adult mouse lemurs (12 males and 4 females) were initially included in this study. Two females that presented brain lesions on anatomical MRI were excluded from the analysis. The 14 analysed animals ranged from 0.9 to 3.1 years old (mean±SD: 1.7±0.7) (Table 1). Housing conditions were cages containing one or two lemurs with jumping and hiding enrichment, temperature 24–26 °C, relative humidity 55% and seasonal lighting (summer: 14 h of light/10 h of dark; winter: 10 h of light/14 h of dark). Food consisted of fresh apples and a homemade mixture of bananas, cereals, eggs and milk. Animals had free access to tap water. None of the animals had previously been involved in pharmacological trials or invasive studies.

2.2. Animal preparation and MRI acquisition

Animals were scanned under isoflurane anaesthesia at 1.25–1.5% in air, with respiratory rate monitored to confirm animal stability until the end of the experiment. Body temperature was maintained by an air heating system at 32 °C, inducing a natural torpor in mouse lemurs (Aujard et al., 2001). This has the advantage of allowing a low anaesthesia level without reawakening. The MRI system was an 11.7 Tesla Bruker BioSpec (Bruker, Ettlingen, Germany) running ParaVision 6.0.1. Each animal was scanned twice with an interval of 6 months. Anatomical images were acquired using a T2-weighted multi-slice multi-echo (MSME) sequence: TR = 5000 ms, TE = 17.5 ms, 6 echoes, inter-echo time = 5 ms, FOV = 32 × 32 mm, 75 slices of 0.2 mm thickness, resolution = 200 µm isotropic, acquisition duration 10 min. Resting state time series data were acquired using a gradient-echo EPI sequence: TR = 1000 ms, TE = 10.0 ms, flip angle = 90°, repetitions = 450, FOV = 30 × 20 mm, 23 slices of 0.9 mm thickness and 0.1 mm gap, resolution = 312 × 208 × 1000 µm, acquisition duration 7 m30 s.

2.3. MRI acquisition in humans

Forty-two healthy participants from the "Imagerie Multimodale de la Maladie d'Alzheimer à un stade Précoce" (IMAP) study (Caen) were included in the present study (18 males and 24 females ranging from 41 to 60 years old (mean±SD: 50.0±5.9)). Detailed inclusion and exclusion criteria can be found in (Chetelat et al., 2008). All subjects lacked abnormality of clinical, MRI, and neuropsychological examinations, as demonstrated by: (1) normal somatic examination, (2) body weight in the normal range, (3) no known vascular risk factor and smoking <10 cigarettes per day, (4) no alcohol or coffee abuse, according to DSM4 criteria, (5) blood pressure within normal limits or corrected to, (6) no history or clinical evidence of sensorineural loss, dementia, or psychiatric disorder (a formal psychiatric interview was not performed), (7) no current use of medication (except birth control pills, oestrogen replacement therapy, anti-hypertensive drugs), and especially no use of centrally acting drugs (sleeping pills, antidepressant drugs) for at least 6 weeks, (8) normal standard T1-, T2- and/or FLAIR-weighted MRI, and notably no significant white matter T2- and FLAIR-weighted hyperintensities. The Mattis dementia rating scale (Mattis, 1976) was used for subjects over 50 years to exclude subjects with scores below the normal range for age indicating potential underlying neurodegenerative pathology. They also underwent cognitive tasks assessing episodic memory, semantic memory and working memory. There was no evidence of significant cognitive decline beyond that expected for normal aging in any subject, and no subject complained about his/her memory. In addition, to ensure that participants were not in the Alzheimer's continuum, we only selected those who had an amyloid-PET scan and in whom the scan revealed no significant amyloid deposition (amyloid-negative). All participants were scanned on a 3.0 T scanner (Philips Achieva, Amsterdam, Netherlands) at the Cyceron Center (Caen, France). Anatomical T1-weighted images were acquired using a 3D fast-field echo sequence (3D-T1-FFE sagittal TR = 20 ms, TE = 4.6 ms, flip angle = 10°, 180 slices of 1 mm with no gap, FOV = 256 × 256 mm^2, in-plane resolution = 1 × 1 mm^2). Resting state time series data were acquired using an interleaved 2D T2* SENSE EPI (2D-T2*-FFE-EPI axial, SENSE = 2; TR = 2382 ms; TE = 30 ms; flip angle = 80°; 42 slices of 2.8 mm with no gap, repetitions = 450, FOV = 224 × 224 mm^2, in-plane resolution = 2.8 × 2.8 mm^2, acquisition duration = 11.5 min). Head motion was minimized with foam pads. Participants were equipped with earplugs and the scanner room's light was turned off. The detailed procedure for fMRI data acquisition and handling is described in Mevel et al. (2013). During this acquisition, which was the last of the MRI scanning session, subjects were asked to relax, lie still in the scanner, and keep their eyes closed while not falling asleep. Immediately after the scanning, the participants were invited to complete a semi-directed questionnaire especially designed for the evaluation of their inner experience during the resting state. No-

tably, the questionnaire allowed to exclude participants who reported falling asleep during the scan, or being in a drowsy state for more than 50% of the resting-state fMRI session (>5 min) and/or showing a constant and focused mental activity about a single thing during the whole session.

2.4. MRI pre-processing

2.4.1. Mouse lemur data

Scanner data were exported as DICOM files then converted into NIfTI-1 format. Then spatial pre-processing was performed using the python module sammba-mri (SmAll MaMmals BrAin MRI; http://sammba-mri.github.io, (Celestine et al., 2020)) which, using nipype for pipelining (Gorgolewski et al., 2011), leverages AFNI (Cox, 1996) for most steps and RATS (Oguz et al., 2014) for brain extraction. Anatomical images were mutually registered to create a study template, which was further registered to a high-resolution anatomical mouse lemur template (Nadkarni et al., 2019). RsfMR images were corrected for slice timing (interleaved), motion, and B0 distortion (per-slice registration to respective anatomicals), then all brought into the same space of the mouse lemur template by successive application of the individual anatomical to study template and study template to mouse lemur atlas transforms. Functional images were further pretreated using Nilearn (Abraham et al., 2014). Nuisance signal regression was applied including a linear trend as well as 24-motion confounds (6 motion parameters, those of the preceding volume, plus each of their squares (Friston et al., 1994)). Images were then spatially smoothed with a 0.9 mm full-width at half-maximum Gaussian filter. The first 10 volumes were excluded from analysis after the preprocessing to ensure steady-state magnetization.

2.4.2. Human data

Artefacts were inspected in individual datasets using the TSDiffAna routines (http://imaging.mrc-cbu.cam.ac.uk/imaging/DataDiagnostics). Datasets displaying significant movements (> 1.5° rotation or > 3 mm translation) and abnormal variance distribution and/or artefacts were excluded from the analysis. Data were then preprocessed as defined in Mutlu et al. (2017) with slice timing correction, realignment to the first volume and spatial normalization within native space to correct for distortion effects. EPI volumes were registered to their own high resolution anatomical image and then registered and normalized to MNI template space. Nuisance signal regression was applied including a linear trend as well as 24-motion confounds (6 motion parameters, those of the preceding volume, plus each of their squares (Friston et al., 1994)). Images were then spatially smoothed with a 2 mm full-width at half-maximum Gaussian filter. Brain regions were classified using the AAL2 atlas ((Rolls et al., 2015; Tzourio-Mazoyer et al., 2002), http://www.gin.cnrs.fr/fr/outils/aal-aal2/, Suppl. Fig. 1). Analyses requiring nodes used 90 regions corresponding to cortical and grey matter subcortical regions without hindbrain.

2.5. 3D functional atlas of mouse lemur brain

The following procedure was used to create a functional atlas of mouse lemur brains. Multi-animal dictionary learning statistical analysis was performed with Nilearn (random_state = 0) (Mensch et al., 2016) on preprocessed rsfMR images. A mask excluding the corpus callosum, hindbrain, ventricles and systematically artefacted regions (olfactory bulb, temporal pole, entorhinal cortex and prepiriform cortex) was used to restrict functional data to non-noisy voxels prior to dictionary learning analysis. During a pilot investigation, several analyses were performed using 20, 30, 35, 40, 45, 50, and 60 sparse components. The study based on 35 sparse components was selected for the final analysis as it highlighted either unilateral local functional regions or bilateral regions that matched well to anatomy (Nadkarni et al., 2019). The 35 sparse components were used to create a 3D functional atlas of the mouse lemur brain. Each bilateral sparse component was split into two unilateral regions. Regions smaller than 5 mm^3 were excluded. Subcortical regions were manually corrected to fit with the current anatomical description of subcortical regions (Nadkarni et al., 2019). This led to a 3D functional atlas presenting with 46 local functional regions that were named using ITK-SNAP (Yushkevich et al., 2006). The name of each structure was defined using the names of brain structures reported in the AAL2 human brain atlas (Rolls et al., 2015; Tzourio-Mazoyer et al., 2002). The definition of each region was based on cytoarchitectonic (Brodmann, 1999 (original in 1909); Le Gros Clark, 1931; Zilles et al., 1979) and anatomical (Bons et al., 1998; Nadkarni et al., 2019) atlases of mouse lemurs as well as AAL2 human brain atlas (Rolls et al., 2015; Tzourio-Mazoyer et al., 2002).

2.6. Identification of large scale networks

2.6.1. Connectivity matrices based on lemur and human atlases

Partial correlation matrices were created using fully preprocessed MR images by calculating the partial correlation coefficients between BOLD MR signal time-courses within each region of the lemur and human 3D atlases. Partial correlations were used because they select direct associations between regions and allow the control of indirect correlations (Mechling et al., 2014). Individual partial correlation matrices were computed from shrunk covariance matrices using the Ledoit and Wolf shrinkage coefficient (Ledoit and Wolf, 2004) as recommended by Varoquaux et al. (2012) and Brier et al. (2015). Partial correlation coefficients were then Fisher's z-transformed. Values from different human subjects or animals were averaged and thresholded based on a one-tailed t-test ($p \leq 0.01$) (Mechling et al., 2014).

In graph theory, large scale networks are defined as community structures (or modules), which are groups of nodes densely interconnected. Several methods have been proposed in order to partition a network into communities (Lambiotte et al., 2015). Here, the number of modules was chosen following pilot investigations based on the "stability of a network partition" method implemented in Gephi 0.9.2 (Bastian et al., 2009) as well as visual evaluation of the obtained networks. The "stability of a network partition" method requires fixing a parameter called "resolution limit of modularity". It imposes a limit on the size of the smallest community obtained by modularity optimisation (Lambiotte et al., 2015). This parameter was set to 0.8 for lemurs and humans leading to partition of lemur and human connectivity matrices into 6 and 8 modules. The modularity of a partition (Q), reflects the degree to which a network can be subdivided into non-overlapping groups of nodes with maximum within-group connections and minimum number of between-group connections (Blondel et al., 2008; Newman, 2006). This parameter, calculated by Gephi 0.9.2, was 0.45 and 0.63 when lemur and human matrices were partitionned into 6 and 8 modules.

2.6.2. Large scale network identification by statistical dictionary learning analysis

Dictionary learning is an analysis that produces network probability maps on concatenated individual records from groups of subjects. Dictionary learning based on a small number of sparse components was performed in mouse lemurs and humans in order to highlight large networks and to compare them. Six and eight sparse components were used in lemurs and humans, respectively, based on the number of modules found with the graph theory analysis. In humans, a mask excluding the hindbrain and white matter was used prior to the analysis to compare the dictionary learning of the two species in a similar space. Dictionary learning produced maps showing voxels belonging to different networks. The generation of these maps does not require any atlas.

2.6.3. Identification of brain regions belonging to large scale networks

3D atlases were used to name the regions belonging to each large scale networks using the following criteria. One region of the 3D atlas was considered to belong to a network if the network occupied at least

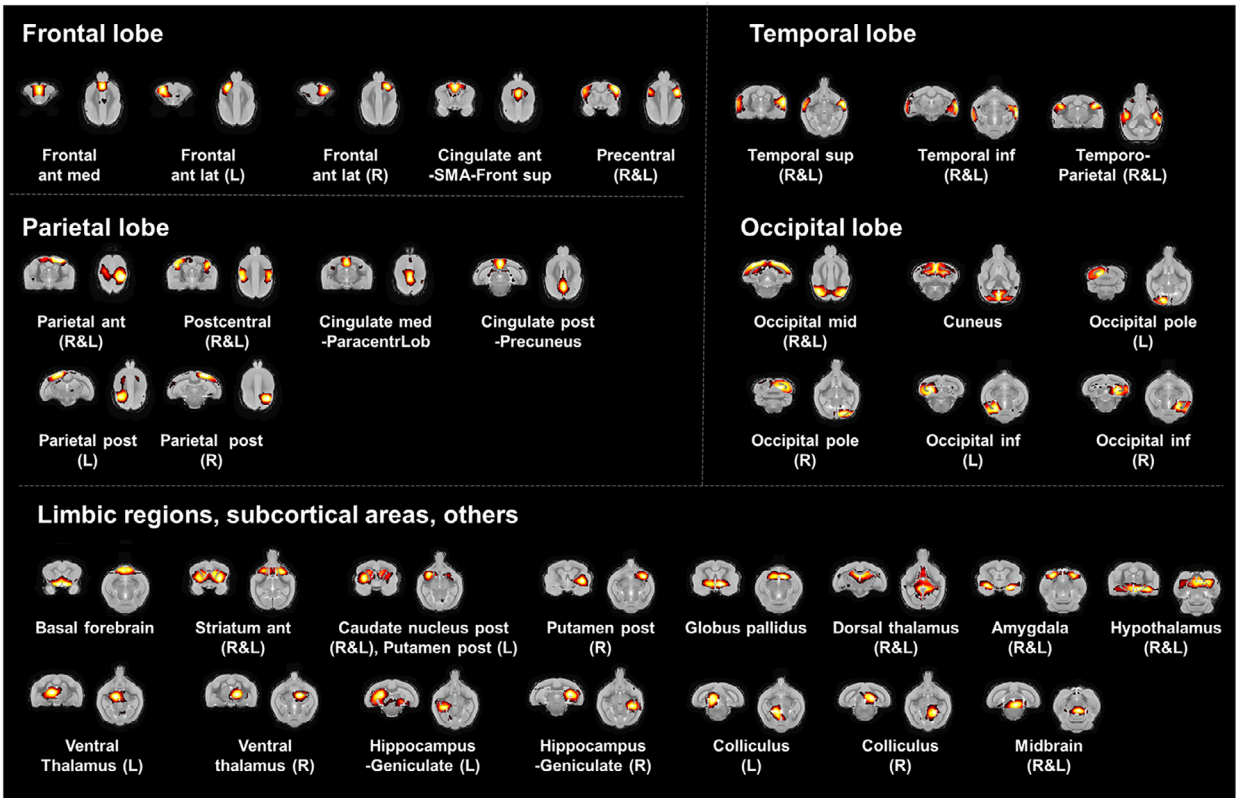

Fig. 1. Functional regions in mouse lemurs. These regions were identified following dictionary learning analyses of rsfMR images using 35 components. They are shown on coronal and axial anatomical templates with an automatic slice selection based on the center of mass of each component.

20% of its volume or if the network represented 120 voxels of this region for mouse lemurs or 200 voxels for humans. Values of 20%, 120 and 200 voxels were arbitrary. In the case of regions that were close to these criteria, bilateralism of the regions was assessed to include only bilateral regions in the networks and exclude unilateral ones. Visual inspection of the maps was always performed to confirm the assignment of brain regions to different networks.

2.7. Evaluation of functional hubness and small-worldness features by graph theory analysis

We consider in this analysis the absolute value of the correlation coefficient as performed routinely in human fMRI graph theory studies (De Vico Fallani et al., 2014).

2.7.1. Hubness

Hubness describes the centrality of nodes in a network and reflects the node influence within the whole brain network. It can be measured by eigenvector centrality. For each node, this index is mainly calculated based on its partial correlation values (edges) with all regions of an atlas, weighted by the eigenvector scores of its neighbourhood nodes. In other words, nodes which display high eigenvector centrality scores are strongly linked to other nodes and/or to strongly connected nodes. Hubness was evaluated in mouse lemur and human brains using eigenvector centrality measures based on NetworkX (Hagberg et al., 2008).

2.7.2. Small-worldness

Network topology was characterized using two small-world coefficients (σ (Watts and Strogatz, 1998) and ω (Telesford et al., 2011)) (NetworkX (Hagberg et al., 2008)).

$$\sigma \text{ is defined as } \sigma = \frac{C/\text{Crand}}{L/\text{Lrand}} \quad \text{(Watts and Strongatz, 1998)}$$

$$\omega \text{ is defined as } \omega = \frac{L}{\text{Lrand}} - \frac{C}{\text{Crand}} \quad \text{(Telesford et al., 2011)}$$

With C and L being, respectively, the average clustering coefficient (a measure of network segregation) and the average shortest path length (a measure of integration) of the network. Crand and Lrand are their equivalent derived random networks. Small-world networks have σ values superior to 1 and ω values close to 0 (Telesford et al., 2011).

3. Results

3.1. Functional atlas of mouse lemur brain

We identified functional regions in mouse lemurs by performing a dictionary learning based on a high number of components (35 sparse components, Fig. 1). Components associated with bilateral structures as shown, for example, for the precentral cortex in Fig. 1 were classified as two different regions (*i.e.* one in each hemisphere). Thus, 46 local functional regions (including 27 cortical regions) could be extracted from the 35-component dictionary analysis (Fig. 2). The name given to these 46 local functional regions as well as their comparison with regions of the human atlas are presented in the Suppl. Table 1. This functional atlas can be downloaded from https://www.nitrc.org/projects/fmri_mouselemur/.

3.2. Cerebral networks in mouse lemurs

Dictionary learning based on six sparse components was then performed to highlight the following large networks (Fig. 3, Fig. 4, Table 2, https://www.nitrc.org/projects/fmri_mouselemur/).

1) The somato-motor network embedded the frontal anterior lateral and all the parietal regions including the precentral (primary motor) and postcentral (primary region involved in body sensation) areas.

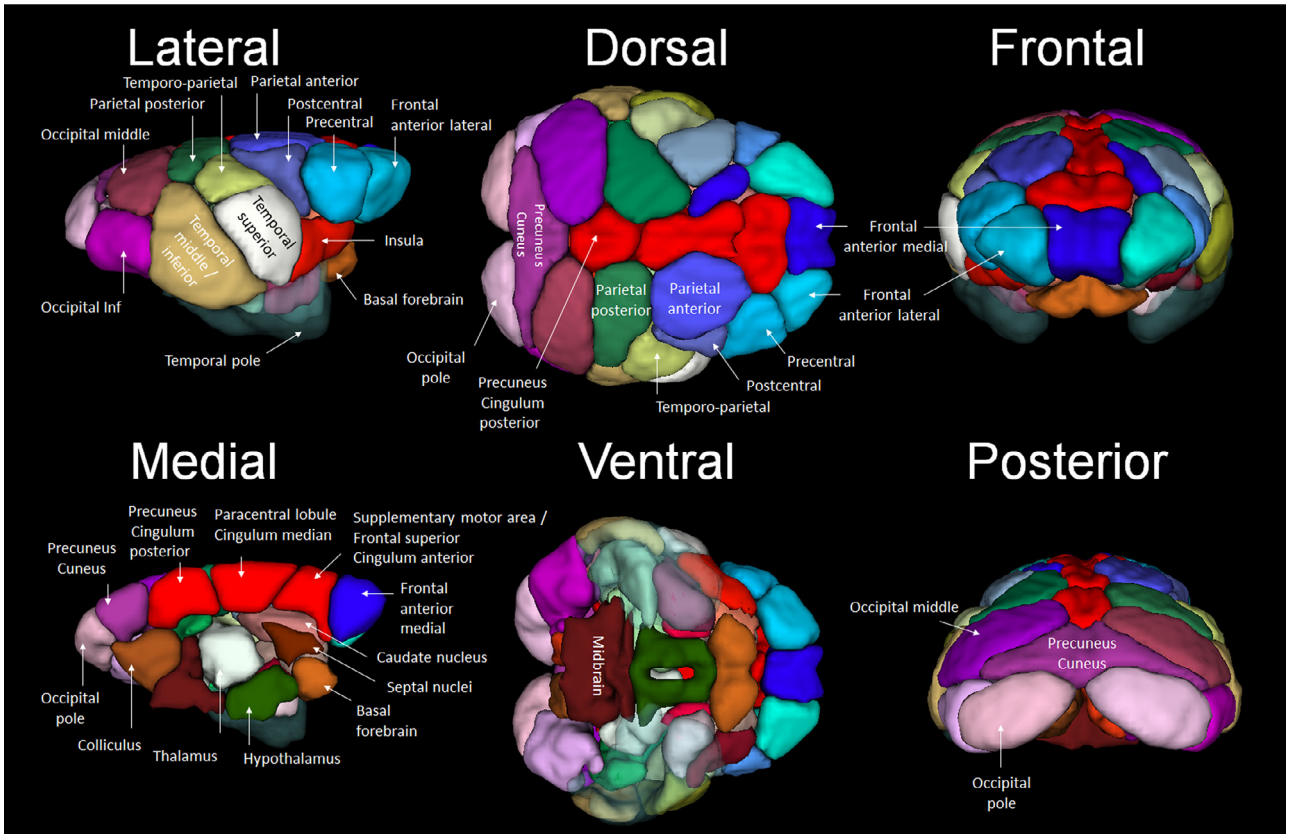

Fig. 2. 3D functional atlas of mouse lemur brain. This atlas was extracted from 46 functional regions identified following dictionary learning analyses of rsfMR images. Temporal pole that could not be included in the analysis is transparent/blue.

It also involved the anterior cingulate cortex/supplementary motor area/frontal superior region, and the medium cingulate/paracentral lobule.

2) The occipito-parietal network involved all the occipital regions as well as regions in the parietal posterior, temporal middle/inferior, and cingulum posterior/precuneus cortices. The strong labelling of occipital and parietal regions evokes the visual network reported in humans (Lee et al., 2012; Raichle, 2011).
3) The fronto-parietal network involved the frontal anterior lateral cortex and dorsal part of the frontal superior medial (dlFC regions), parietal posterior cortex, medial and posterior cingulate cortices as well as retrosplenial regions (classified as cingulum posterior/precuneus and precuneus/cuneus in our atlas). It also embedded temporal middle/inferior cortex, hippocampus, and occipital regions (Figs. 3–4, Table 2).
4) The fronto-temporal network involved the frontal anterior medial and lateral regions, the precentral cortex, all the temporal regions, the parietal posterior cortex, the anterior and medial cingulum cortices, and the insular cortex.
5) The sensory-limbic network involved limbic structures (basal forebrain, septal nuclei, midbrain, hippocampus, hypothalamus) and a large number of regions involved in vision (occipital cortex, superior colliculi) or audition (inferior colliculi). It also embedded the cingulum posterior/precuneus and subcortical regions (thalamus, caudate nucleus and the globus pallidus).
6) The evaluative-limbic network embedded limbic structures (basal forebrain, septal nuclei, amygdala, hippocampus), the insula, as well as subcortical structures (striatum including the caudate nucleus, putamen and the accumbens nucleus of the ventral striatum, and the globus pallidus).

3.3. Cerebral networks in humans

Human resting state networks have been described in great detail in several articles. Here, the method used in lemurs was applied to a human dataset mainly to evaluate its ability to detect relevant networks. The human functional matrix was segregated into 8 modules that were used to further characterize large scale networks using dictionary learning. The 8 networks were classified using information from the literature and indeed revealed well characterized human networks (Fig. 4, Suppl. Fig. 2, Suppl. Table 2). For example, the DMN was identified based on its three core clusters: i. the medial frontal cortex (mFC), ii. the medial parietal (*i.e.* precuneus region) and posterior cingulate/retrosplenial cortices, and iii. the parietal and angular cortices (Lee et al., 2012; Liu et al., 2019; Raichle, 2011). Some other clusters usually associated with these core clusters (Liu et al., 2019) were also detected: lateral frontal regions (dorso-lateral frontal cortex (dlFC)), anterior (and to a lower extent medial) cingulate regions, temporal and occipital regions. The 7 other networks identified were the dorsal fronto-parietal (classified as dorsal attention network (DAN) in (Corbetta and Shulman, 2002; Hopfinger et al., 2000; Lee et al., 2012)), fronto-supramarginal (Lee et al., 2012) (classified as executive control network (ECN) in (Raichle, 2011; Sole-Padulles et al., 2016)), somato-motor (Lee et al., 2012; Raichle, 2011), fronto-temporal (classified as ventral attention network in (Farrant and Uddin, 2015; Lee et al., 2012)), occipito-parietal network classified as visual network in (Lee et al., 2012; Raichle, 2011). This latter network corresponded mainly to the dorsal stream of the visual network (Migliaccio et al., 2016). We also detected an occipito-temporal network that could correspond to the ventral part of the visual network (Migliaccio et al., 2016). Finally, the salience network was identified (Goulden et al., 2014; Lee et al., 2012; Zhou et al., 2018).

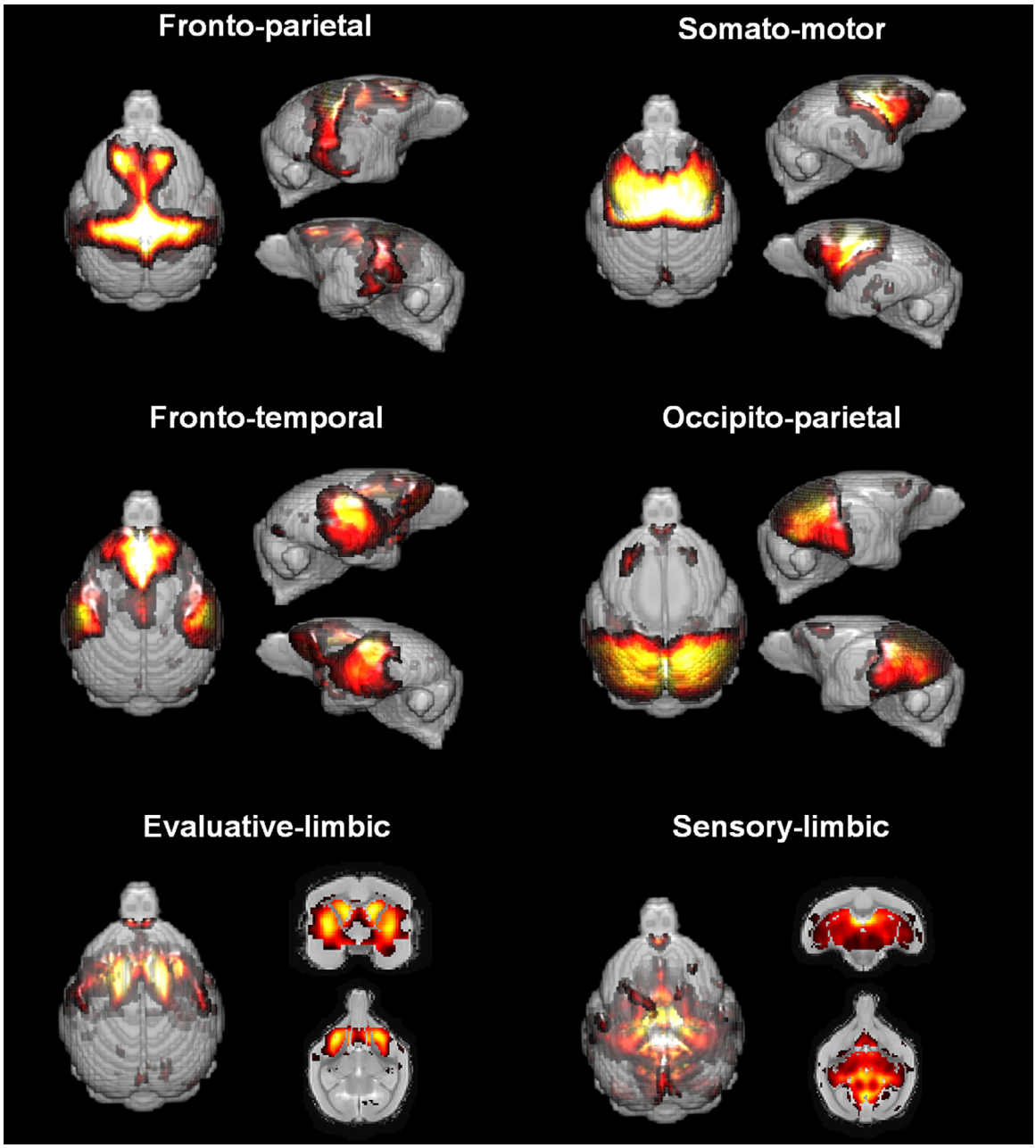

Fig. 3. Cerebral networks identified in mouse lemurs. These bilateral networks were classified as fronto-parietal, somato-motor, fronto-temporal, occipito-parietal, evaluative-limbic, and sensory-limbic networks.

3.4. Functional hubs and small-worldness features of mouse lemur and human brains

3.4.1. Brain hubs in mouse lemurs and humans

Hubness describes the centrality of nodes in a network and reflects the node influence within the whole brain network. It can be measured by eigenvector centrality. In mouse lemurs, the main hubs were all connected together along the rostro-caudal axis (Fig. 5A, Suppl. Table 3). The nodes presenting the highest eigenvector centrality were the medial, posterior, and anterior cingulum cortices, the anterior and posterior parietal cortices, the temporo-parietal cortex as well as the postcentral cortex (Fig. 5A, Suppl. Table 3). All these regions that are part of the 10 strongest hubs belong to the fronto-parietal, fronto-temporal and somato-motor networks. In humans, the three nodes presenting the highest eigenvector centrality were localized in the integrative parietal regions (angular, precuneus and inferior parietal cortices) (Fig. 5B, Suppl. Table 4). Then the next hubs were localized in the frontal cortex (frontal inferior orbital, middle frontal, frontal superior medial, and frontal superior cortices). All these regions that are part of the 10 strongest hubs belong to the DMN. There was a lack of spatial continuity between the hubs distributed within parietal and frontal clusters. A striking difference between hubs of lemurs and humans was the involvement of the cingulate cortices in mouse lemurs and not in humans.

3.4.2. Small-worldness of mouse lemur and human brain networks

Network topology describes properties of regional specialization and global information transfer efficacy of a network. Three main classes of networks have been described: random, lattice and small-world networks (Telesford et al., 2011). Usually, mammal brains have small-world properties (Mechling et al., 2014), which is an optimal organization for local information processing in specialized regions and for

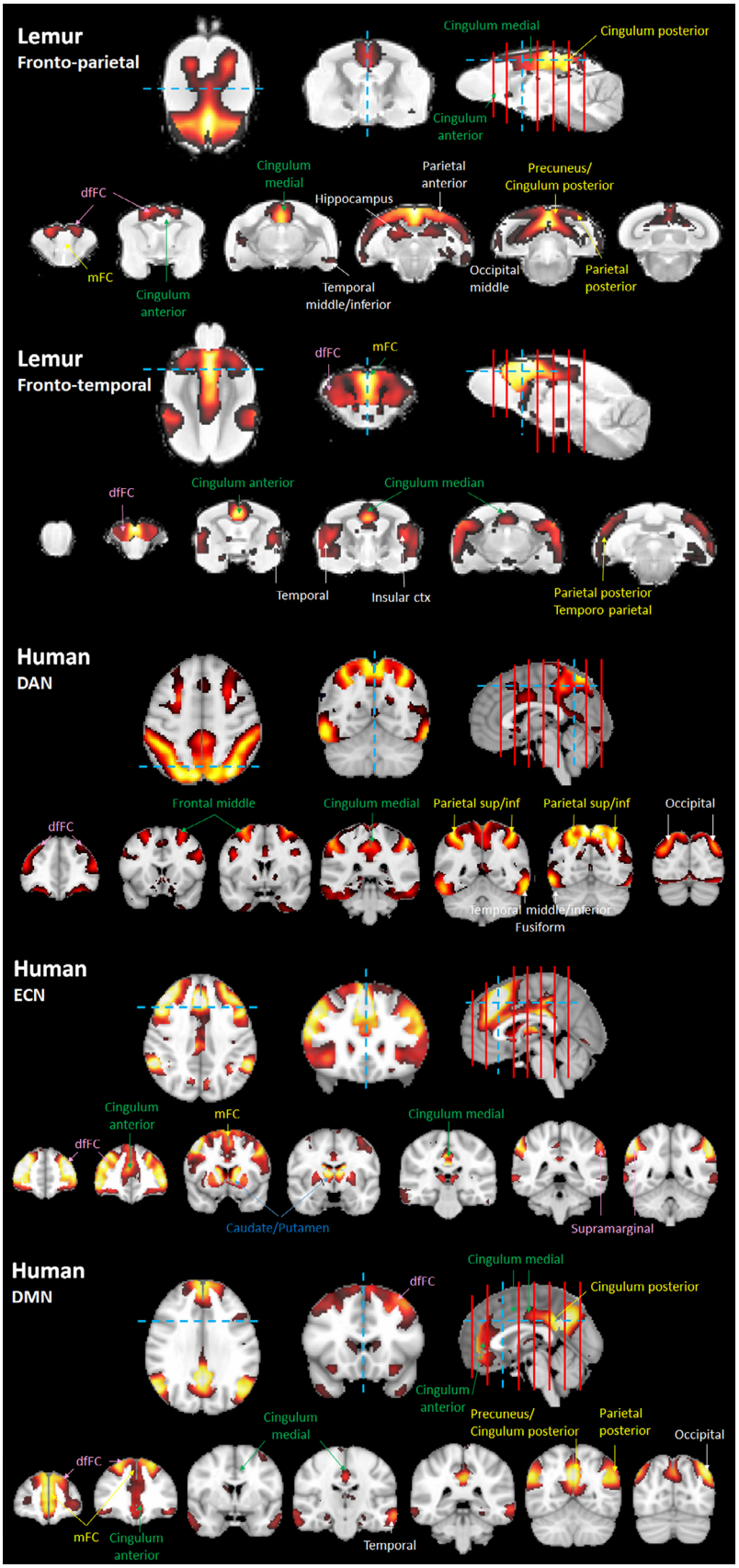

Fig. 4. Comparison of fronto-parietal and fronto-temporal networks in mouse lemurs to **dorsal attentional (DAN), executive control (ECN), and default mode (DMN) networks in humans.** The fronto-parietal network of the mouse lemurs embedded the frontal anterior lateral cortex and dorsal part of the frontal superior medial (dlFC regions), parietal posterior cortex, medial and posterior cingulate cortices as well as the precuneus. It also embedded temporal middle/inferior cortex, hippocampus, and occipital regions. The fronto-temporal network of mouse lemurs embedded the frontal anterior medial and lateral regions (dlFC and mFC regions), temporal regions, the parietal posterior cortex, the anterior and medial cingulum cortices, and the insular cortex. These networks presented similarities with human networks than can be identified based on their core clusters. The DAN that embeds the dlFC, the medial cingulate, the parietal, the middle and inferior temporal, and the occipital cortices. The ECN that embeds the dlFC and parietal supramarginal regions (labelled in pink). The DMN that embeds the mFC, medial parietal (*i.e.* precuneus region) and posterior cingulate/retrosplenial cortices, the parietal and angular cortices as core clusters (labelled in yellow). It also involved other regions as the dlFC, anterior and medial cingulate cortices, temporal and occipital regions.

Table 2
Brain regions of mouse lemurs participating to different networks. Regions belonging to one of the top fifteen hubs are presented with bold letters. Detail of the regions involved in the different networks is also presented: mFC: medial frontal cortex; dlFC: dorso-lateral frontal cortex. SMA: supplementary motor area; PreC: precuneus.

	Label name	Fronto-parietal	Fronto-temporal	Somato-motor	Visual	Sensory limbic	Evaluative limbic
Frontal and precentral	**Frontal anterior medial**		**X**				
	Frontal anterior lateral	**X** (dlFC)	**X**	**X**			
	Precentral		**X**	**X**			
	+ Frontal inferior triangularis part						
	+ Frontal inferior opercular part						
	+ Rolandic operculum						
Cingulum Precuneus	**Cingulum anterior**	**X** (dlFC)	**X**	**X** (SMA)			
	+ Frontal superior medial						
	+ Supplementary motor area						
	Cingulum median	**X**	**X**	**X**			
	+ Paracentral lobule						
	Cingulum posterior	**X**			**X**	**X**	
	+ Precuneus				(PreC)		
	Precuneus	**X**			**X**	**X**	
	+ cuneus						
Insular	Insular cortex		**X**				**X**
Parietal	**Postcentral**			**X**			
	Parietal anterior			**X**			
	Parietal posterior	**X**	**X**	**X**	**X**		
Temporal	**Temporo-parietal**		**X**	**X**			
	Temporal superior		**X**				**X**
	Temporal middle / inferior	**X**	**X**		**X**		
Occipital	Occipital middle	**X**			**X**		
	Occipital inferior				**X**	**X**	
	Occipital pole				**X**		
Limbic regions	Hippocampus	**X**				**X**	+/-
	Amygdala						**X**
	Basal forebrain					**X**	**X**
	Septal nuclei					**X**	**X**
	Hypothalamus					**X**	
Subcortical regions	Caudate nucleus					**X**	**X**
	Putamen						**X**
	Globus pallidus					**X**	**X**
	Thalamus					**X**	
Others	Colliculus					**X**	
	Midbrain					**X**	

its global transfer to share the processed information in communicating regions to further process it (Telesford et al., 2011). Network topology can be characterized using two small-world coefficients (σ and ω) (Hagberg et al., 2008). Small-world networks have σ values superior to 1 and ω values close to 0 (Telesford et al., 2011). As expected we found small-world properties in mouse lemur and human brains (σ = 1.48 and 1.20 and ω = 0.46 and 0.53).

4. Discussion

RsfMRI was used to characterize functional cerebral regions, neuronal networks, and hubs of mouse lemur primates.

4.1. Functional atlas of mouse lemur brain

After the seminal work of Brodmann (1999 (original in 1909)), cytoarchitectural and other histology-based labeling techniques were the standard methods for brain parcellation and, up to now, description of mouse lemur functional organisation was relied on these methods (Bons et al., 1998; Le Gros Clark, 1931; Nadkarni et al., 2019; Zilles et al., 1979). New techniques of brain parcellation based on task-associated functional MRI or resting-state functional MRI are now used in humans (Craddock et al., 2012; Glasser et al., 2016; Yeo et al., 2011) and animals (Liang et al., 2011). Here, using dictionary learning with a large number of components, we created a 3D atlas showing 46 functional regions. No predetermined anatomical atlas was required during the creation of this atlas. In association with the evaluation of functional cerebral networks, this analysis provides the capacity to evaluate brain organization in precious species. Functional atlases are highly relevant as they were shown to be superior to anatomical atlases to define functionally homogeneous regions of interest (Craddock et al., 2012). In the case of mouse lemurs, the two published atlases of cortical regions based on cytoarchitectony display major discrepancies (Le Gros Clark, 1931; Zilles et al., 1979). For example, in Zilles atlas the somatosensorial cortex (Brodmann 1-3) and the primary motor cortex (Brodmann 4) follow a ventro-dorsal axe, while they follow a postero-anterior axe in Le Gros Clark atlas. Our functional atlas suggests that they follow a ventro-dorsal axe, consistently with what was suggested by Zilles. Likewise the caudal border of the primary motor area is in a more posterior position in Le Gros Clark than in Zilles atlas and our functional atlas is consistent with Zilles description. More interestingly, our atlas shows that the most rostral part of the frontal lobe is functionally separated from the motor frontal region and thus probably represents the mouse lemur prefrontal cortex, which had never been described until now.

4.2. Primary cortical networks

Here we outlined four cortical networks in lemurs. Two of them (somato-motor and occipito-parietal (visual)) were highly similar in mouse lemurs and humans. They are also identified in several species from rodents (Grandjean et al., 2017) to primates (Belcher et al., 2013). In evolutionary science, homology is defined as structural or functional similarities derived from common ancestry (Deacon, 1990), and we considered that these networks are homologous in lemurs and humans.

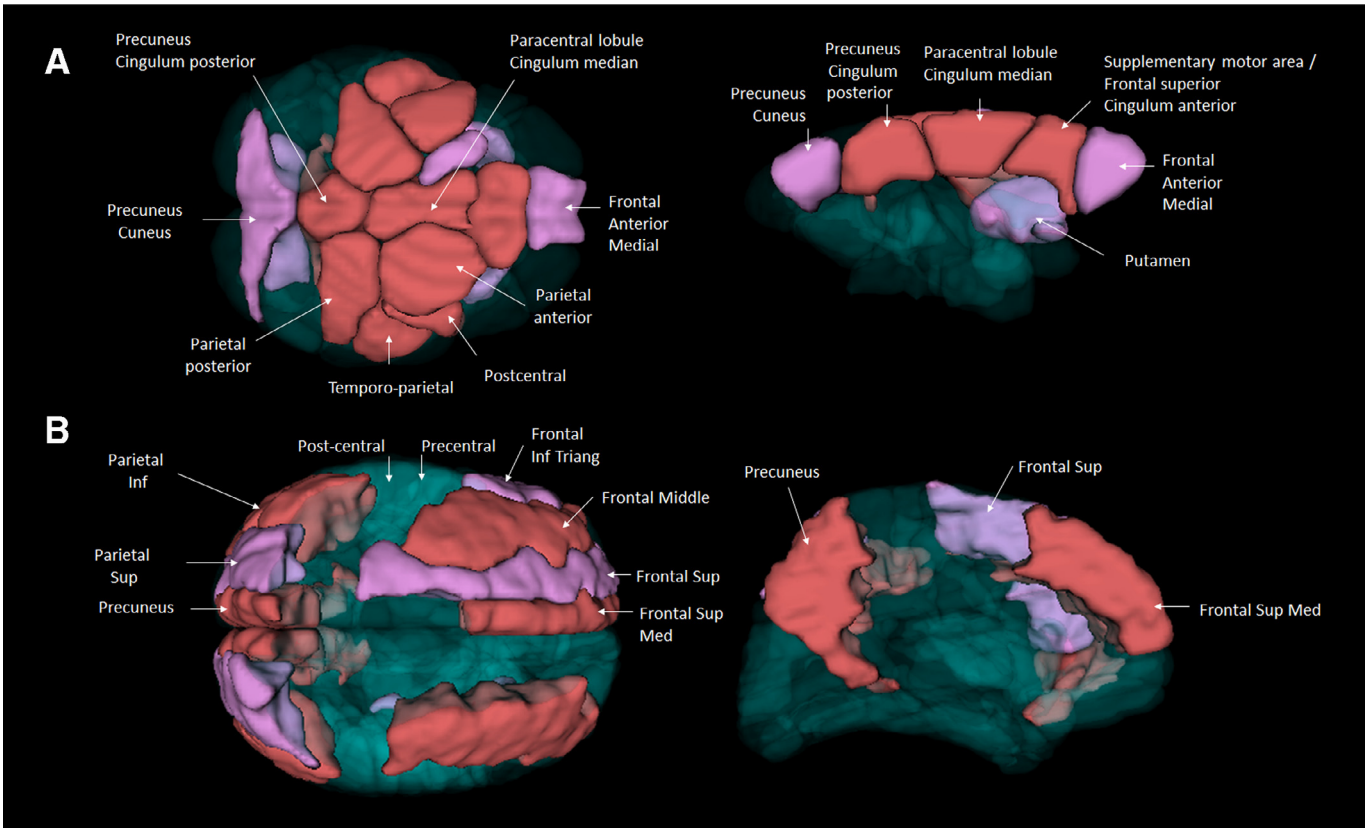

Fig. 5. Comparison of major hubs in mouse lemurs and humans. For each species, the 10 strongest hubs are displayed in red and the 5 following strongest hubs are labelled in pink. Other brain regions are blue/transparent.

4.3. High level cortical networks

The fronto-parietal and fronto-temporal networks were two other cortical networks identified in mouse lemurs. Most of the regions associated to the fronto-parietal network (frontal anterior lateral cortex and dorsal part of the frontal superior medial (dlFC regions), parietal posterior cortex (pPC), medial cingulate cortex, precuneus/cuneus, temporal middle/inferior cortex, and occipital regions) are the ones that characterize the human DAN network as reported by Corbetta and Shulman (2002), Hopfinger et al. (2000) or our study (Suppl. Table 2, Fig. 4). So it is tempting to assume a partial homology between the mouse lemur fronto-parietal network and the human DAN. This network however also presents some regions that are not usually associated to the human DAN (hippocampus and posterior cingulate cortex (pCC)) but are key regions of the DMN. It also involved another key regions of the human DMN *i.e.* the pPC (Liu et al., 2019). Thus, as an alternative hypothesis, the fronto-parietal network could be compared to the human DMN. One major difference is however that in humans the DMN is also characterized by the mFC (Liu et al., 2019), a region that was not detected in mouse lemur fronto-parietal network. In a network identified as DMN-like in several primates, the mFC is either absent as in marmosets (Liu et al., 2019) or much smaller than that of human DMN as in macaques (Mantini et al., 2011). Interestingly, the main frontal region involved in the DMN-like network of marmoset or macaques is the dlFC (Liu et al., 2019; Mantini et al., 2011). This region was also the main frontal region involved in mouse lemur fronto-parietal network. The fronto-parietal network identified in lemurs could thus be a network similar to the "mFC-free" DMN-like network identified in other primates. One of the characteristics of the human DMN or of the DMN-like network of marmosets or macaques is that they are deactivated during functional tasks. Future studies should thus evaluate the activity of the mouse lemur fronto-parietal network during functional task. In the absence of perfect homology between lemur fronto-parietal network and human networks, one can propose hypotheses on the function of the lemur network based on its anatomical regions. This fronto-parietal network involves critical regions for visual function (occipital and inferior temporal), for spatial processing and action in space (parietal posterior, precuneus, posterior cingulate regions, hippocampus), as well as for motor function (dorso-lateral frontal cortex, supplementary motor area) (Fattori et al., 2017; Jacobs and Schenk, 2003; Rolls, 2019; Snyder et al., 1997). Thus, our hypothesis is that the lemur fronto-parietal network subserves visuo-spatial function leading to motor activity, *i.e.* control of actions based on exteroceptif visuo-spatial stimuli.

The fronto-temporal network is the second high-level network in mouse lemurs. It is composed of the frontal anterior medial and lateral regions, the precentral cortex, all the temporal regions, the parietal posterior cortex, the anterior to mid cingulate, and the insular cortex. This network may be partly homologous with the human ECN. Indeed, both networks cover the mFC, dlFC, part of the parietal cortex, the anterior/medial cingulate cortices and the insula ((Beckmann et al., 2005; Sole-Padulles et al., 2016), Fig. 4). As an alternative hypothesis, the mouse lemur fronto-temporal network could be compared to the human DMN as it displayed two of the DMN core clusters *i.e.* the mFC and the parietal posterior cortex. However, the posterior cingulate cortex, another core region of the human DMN is not part of the lemur fronto-temporal network. We also identified similarities between the mouse lemur fronto-temporal network and the human salience network because of the presence of insula, cingulate and temporal regions in both networks. Finally, the mouse lemur fronto-temporal network can obviously be compared to the human fronto-temporal network, as they both embed fronto-temporal cortices and the insula. In the absence of perfect homology between lemur fronto-temporal network and hu-

man networks, we also propose hypotheses on the function of the lemur network based on its anatomical regions. Several regions of the mouse lemur fronto-temporal network (medial frontal, the anterior to mid cingulate and the insular cortex) are the core regions involved in an "interoceptive system" (Barrett and Simmons, 2015). This system modulates attentional, sensory and behavioral responses to homeostatically relevant stimuli, as autonomic and hormonal changes (Barrett and Simmons, 2015). Thus, our hypothesis is that the lemur fronto-temporal network is involved in self-referential decisions. As for many complex networks, this hypothesis does not rule out its implication in many other functions.

4.4. Limbic networks

Two networks, involving the limbic system, were found in lemurs. The first one (sensory-limbic) embedded regions involved in visual and auditory sensory input, the hypothalamus (implicated in the regulation of endocrine and autonomic systems) as well as brain structures (basal forebrain, septum and midbrain) that contain ascending excitatory cholinergic neurons involved in arousal due to sensory input (Knudsen, 2011; Wenk, 1997). It also involved nuclei of the basal ganglia (caudate nucleus, globus pallidus) involved in the processing of movement-related information. Our hypothesis is that these structures could form a bottom-up arousal system in response to sensory stimuli. The second limbic network (evaluative-limbic) also comprised brain structures with ascending excitatory cholinergic neurons (basal forebrain, septum) as well as the basal ganglia (caudate nucleus, globus pallidus, putamen). It also involved the amygdala and the insula. The amygdala processes information about the positive/negative valence of stimuli and, in particular via its connections with the basal ganglia, can bias behaviors in an adaptive manner (Janak and Tye, 2015). The insula is involved in the perception of the physiological condition of the body and transmits signals regarding the bodily states to guide emotion and behavior (Bechara, 2005; Craig, 2002). Thus, both the amygdala and the insula are implicated in evaluative, motivational and affective processing (Berntson et al., 2011). Our hypothesis is that this network could subserve behavioral responses to the positive/negative valence of stimuli as well as to the internal state of the body. Although we did not detect them in our analysis, human networks involving the basal ganglia that resemble the evaluative-limbic network are reported in (Sierakowiak et al., 2015; Wen et al., 2012). Limbic networks are also reported in macaques (Hutchison et al., 2012).

4.5. Cerebral hubs

Brain networks are organized around hubs that are integrators of segregated brain systems. Hubs are critical for efficient brain functions and are also points of vulnerability susceptible to disconnection and dysfunction in brain disorders. The strongest cortical hubs of mouse lemurs were grouped along a dorsal antero-posterior axis and involved frontal anterior medial, whole cingulate and parietal cortices. Mice (Liska et al., 2015), rats (D'Souza et al., 2014), and marmosets (Belcher et al., 2016; Ghahremani et al., 2017) display a similar antero-posterior organization of cortical hubs. In humans, the literature suggests that hubs are split into distinct parietal and frontal clusters (Ardesch et al., 2019; Li et al., 2013; Miranda-Dominguez et al., 2014; van den Heuvel and Sporns, 2013). Our results in humans are consistent with this literature. The splitting of hubs into frontal and posterior (retrospenial/parietal) clusters is also described in macaques and chimpanzees (Li et al., 2013), which led to the hypothesis that cerebral network evolution is associated with the occurrence of non-contiguous clusters of associative multimodal regions connected by hubs (Ardesch et al., 2019; Buckner and Krienen, 2013). Splitting cerebral modules into different brain regions connected by strong hubs may be an efficient way to integrate information processed by distant associative regions. The splitting of hubs into distinct clusters is, however, not a primate characteristic, as it was not found in marmosets or mouse lemurs. This might be a characteristic of larger brains, that arose to reduce wiring cost while maximize topological integration in large brains (van den Heuvel et al., 2016).

Mouse lemur hubs also involved subcortical structures (*i.e.* the putamen). This is similar to data in marmosets in which putamen, caudate and thalamus were reported as hubs (Belcher et al., 2016).

4.6. Limitations and perspectives

This study is the first to describe neuronal networks in a strepsirrhine primate. It was based on images recorded with the highest magnetic field ever used in primates (11.7 Tesla) to provide highly sensitive images. It was conducted on sedated animals, although we used the lowest possible non-awakening isoflurane level (1.25%). Compared to wake state, anaesthesia induces a poorer repertoire of functional configurations (Barttfeld et al., 2015), small topological changes, such as reduced (but not supressed) detection of the posterior cingulate cortex within the DMN (Greicius et al., 2008) or lack of detection of frontal regions in the DMN (Hori et al., 2020). Changes in thalamic connectivity have also been reported during isoflurane anaesthesia (Hori et al., 2020). However, when rsfMR images are recorded across a long time period, as done in our study, several studies reported that general patterns of functional brain activity and the number of detected resting-state networks are globally similar in wake and anaesthesia state, including under isoflurane (Barttfeld et al., 2015; Hori et al., 2020; Vincent et al., 2007). Also several high level cortical networks (*e.g.* the fronto-parietal or fronto-temporal) were detected in lemurs and were close to networks reported in awake marmosets (*e.g.* the DMN-like network reported in (Liu et al., 2019)). Thus, although we cannot rule out that some of the networks reported in anaesthetised lemurs are different than the one that would be detected in awake animals, the differences are not expected to be major. Some studies in rats however reported that under isoflurane, cortico-cortical functional connectivity is stronger than during wake state and that isoflurane induces synchronous striato-cortical fluctuations. In addition to masking functional connectivity in some networks (Paasonen et al., 2018), this effect could lead to the detection of false positive resting state networks during isoflurane anaesthesia as compared to the wake state. Further studies are now required to confirm the results obtained in this first study in particular in wake animals.

The dictionary method used to characterize networks requires an a priori selection of the number of components the observer wishes to extract. Due to the gradualness of the interactions between the different regions of the brain, there are no absolute boundaries between large scale networks and several methods have been proposed in order to partition a network into communities (Blondel et al., 2008; Lambiotte et al., 2015). Thus the number of networks selected in a resting state study can be seen as "arbitrary". Here, the number of networks identified in lemurs and humans was based on the same method ("stability of a network partition" method implemented in Gephi 0.9.2). Increasing the number of networks would have split some networks into subnetworks (Yeo et al., 2011).

Another limitation of our study concerns the functional interpretation of the networks reported in lemurs. Studies in wake or in stimulated animals will have to be performed in the future to explore the function of the networks identified in lemurs. In particular, as the characterization of DMN networks relies on its deactivation by task-based fMRI, it will be critical to perform such study in lemurs. This experiment is however beyond the scope of the current article.

5. Conclusion

This study provides the first functional atlas of mouse lemur brains and the first characterisation of functional brain networks and hubs in this primate. By comparing networks and hubs in lemurs and humans, we could identify homologies for the somato-motor and visual cortical networks. The fronto-parietal and fronto-temporal higher order net-

works found in lemurs were not homologous to human networks but displayed similarities with some of them as the DAN, ECN, or DMN. Limbic networks were detected in lemurs. This is consistent with the view that high level networks have evolved in primates and that this evolution is associated to differential organization of regions that are associated to the DAN, ECN and DMN networks (Dixon et al., 2018).

Acknowledgments

We thank everyone who contributed to IMAP+ data acquisition and analyses: Florence Mézenge, Renaud La Joie, Julie Gonneaud, Audrey Perrotin, Robin de Flores, Clémence Tomadesso, Justine Mutlu, Nicolas Villain, Marine Fouquet, Katell Mevel, Francis Eustache, Béatrice Desgranges, Stéphanie Egret, Vincent de La Sayette, Fausto Viader, Alice Pélerin, Malo Gaubert, Géraldine Poisnel, Anne Quillard, Ahmed Abbas, Louisa Barré, Alain Manrique, Florence Pasquier, the Cyceron staff members; and the volunteers who were included in this study.

Credit Author Statement

Clément M. Garin: Conceptualization, Methodology, Software, Validation, Formal analysis, Investigation, Resources, Data Curation, Writing - Original Draft, Writing - Review & Editing, Visualization, Supervision

Nachiket A. Nadkarni: Conceptualization, Methodology, Software, Validation, Formal analysis, Investigation, Resources, Data Curation, Writing - Review & Editing

Brigitte Landeau: Validation, Formal analysis, Investigation, Resources, Data Curation

Gaël Chételat: Conceptualization, Validation, Formal analysis, Investigation, Resources, Data Curation, Writing - Review & Editing, Supervision, Project administration, Funding acquisition

Jean-Luc Picq: Writing - Original Draft, Writing - Review & Editing

Salma Bougacha: Conceptualization, Methodology, Software, Validation, Formal analysis, Investigation, Resources

Marc Dhenain: Conceptualization, Methodology, Software, Validation, Formal analysis, Investigation, Resources, Data Curation, Writing - Original Draft, Writing - Review & Editing, Visualization, Supervision, Project administration, Funding acquisition

Funding

This work was supported by France-Alzheimer Association, Plan Alzheimer Foundation, the French Public Investment Bank's "ROMANE" program, Neuratris, and the CEA bottom-up program.

Supplementary materials

Supplementary material associated with this article can be found, in the online version, at doi:10.1016/j.neuroimage.2020.117589.

References

Abraham, A., Pedregosa, F., Eickenberg, M., Gervais, P., Mueller, A., Kossaifi, J., Gramfort, A., Thirion, B., Varoquaux, G., 2014. Machine learning for neuroimaging with scikit-learn. Front. Neuroinform. 8. doi:10.3389/fninf.2014.00014.

Ardesch, D.J., Scholtens, L.H., Li, L.C., Preuss, T.M., Rilling, J.K., van den Heuvel, M.P., 2019. Evolutionary expansion of connectivity between multimodal association areas in the human brain compared with chimpanzees. Proc. Natl. Acad. Sci. USA 116, 7101–7106. doi:10.1073/pnas.1818512116.

Aujard, F., Dhkissi-Benyahya, O., Fournier, I., Claustrat, B., Schilling, A., Cooper, H.M., Perret, M., 2001. Artificially accelerated aging by shortened photoperiod alters early gene expression (Fos) in the suprachiasmatic nucleus and sulfatoxymelatonin excretion in a primate. Neuroscience 105, 403–412. doi:10.1016/S0306-4522(01)00202-0.

Barrett, L.F., Simmons, W.K., 2015. Interoceptive predictions in the brain. Nat. Rev. Neurosci. 16, 419–429. doi:10.1038/nrn3950.

Barttfeld, P., Uhrig, L., Sitt, J.D., Sigman, M., Jarraya, B., Dehaene, S., 2015. Signature of consciousness in the dynamics of resting-state brain activity. Proc. Natl. Acad. Sci. USA 112, 887–892. doi:10.1073/pnas.1418031112.

Bassett, D.S., Sporns, O., 2017. Network neuroscience. Nat. Neurosci. 20, 353–364. doi:10.1038/nn.4502.

Bastian, M., Heymann, S., Jacomy, M., 2009. Gephi: an open source software for exploring and manipulating networks. International AAAI Conference on Weblogs and Social Media https://www.aaai.org/ocs/index.php/ICWSM/09/paper/view/154 doi:10.13140/2.1.1341.1520.

Bechara, A., 2005. Decision making, impulse control and loss of willpower to resist drugs: a neurocognitive perspective. Nat. Neurosci. 8, 1458–1463. doi:10.1038/nn1584.

Beckmann, C.F., DeLuca, M., Devlin, J.T., Smith, S.M., 2005. Investigations into resting-state connectivity using independent component analysis. Philos. Trans. R. Soc. Lond. 360, 1001–1013. doi:10.1098/rstb.2005.1634.

Belcher, A.M., Yen, C.C., Notardonato, L., Ross, T.J., Volkow, N.D., Yang, Y., Stein, E.A., Silva, A.C., Tomasi, D., 2016. Functional connectivity hubs and networks in the awake marmoset brain. Front. Integr. Neurosci. 10, 9. doi:10.3389/fnint.2016.00009.

Belcher, A.M., Yen, C.C., Stepp, H., Gu, H., Lu, H., Yang, Y., Silva, A.C., Stein, E.A., 2013. Large-scale brain networks in the awake, truly resting marmoset monkey. J. Neurosci. 33, 16796–16804. doi:10.1523/JNEUROSCI.3146-13.2013.

Berntson, G.G., Norman, G.J., Bechara, A., Bruss, J., Tranel, D., Cacioppo, J.T., 2011. The insula and evaluative processes. Psychol. Sci. 22, 80–86. doi:10.1177/0956797610391097.

Biswal, B., Yetkin, F.Z., Haughton, V.M., Hyde, J.S., 1995. Functional connectivity in the motor cortex of resting human brain using echo-planar MRI. Magn. Reson. Med. 34, 537–541. doi:10.1002/mrm.1910340409.

Blondel, V.D., Guillaume, J.L., Lambiotte, R., Lefebvre, E., 2008. Fast unfolding of communities in large networks. J. Stat. Mech.-Theory E doi:10.1088/1742-5468/2008/10/P10008.

Bons, N., Sihol, S., Barbier, V., Mestre-Frances, N., Albe-Fessard, D., 1998. A stereotaxic atlas of the grey lesser mouse lemur brain (*Microcebus murinus*). Brain Res. Bull. 46, 1–173. doi:10.1016/S0361-9230(97)00458-9.

Brier, M.R., Mitra, A., McCarthy, J.E., Ances, B.M., Snyder, A.Z., 2015. Partial covariance based functional connectivity computation using Ledoit-Wolf covariance regularization. Neuroimage 121, 29–38. doi:10.1016/j.neuroimage.2015.07.039.

Brodmann, K., 1999. Brodmann's Localisation in the Cerebral Cortex [Vergleichende Lokalisationslehre der Grosshirnrinde in ihren Orinzipien Dargestellt auf Grund des Zellenbaus]. Imperial College Press, London Garey, Laurence J. ed. (original in 1909).

Buckner, R.L., Krienen, F.M., 2013. The evolution of distributed association networks in the human brain. Trends Cogn. Sci. 17, 648–665. doi:10.1016/j.tics.2013.09.017.

Celestine, M., Nadkarni, N.A., Garin, C., Bougacha, S., Dhenain, M., 2020. Sammba-MRI, a library for small animal neuroimaging data processing in Python. Front. NeuroInform. 14, 24. doi:10.3389/fninf.2020.00024.

Chetelat, G., Fouquet, M., Kalpouzos, G., Denghien, I., De la Sayette, V., Viader, F., Mezenge, F., Landeau, B., Baron, J.C., Eustache, F., Desgranges, B., 2008. Three-dimensional surface mapping of hippocampal atrophy progression from MCI to AD and over normal aging as assessed using voxel-based morphometry. Neuropsychologia 46, 1721–1731. doi:10.1016/j.neuropsychologia.2007.11.037.

Corbetta, M., Shulman, G.L., 2002. Control of goal-directed and stimulus-driven attention in the brain. Nat. Rev. Neurosci. 3, 201–215. doi:10.1038/nrn755.

Cox, R.W., 1996. AFNI: software for analysis and visualization of functional magnetic resonance neuroimages. Comput. Biomed. Res. 29, 162–173. doi:10.1006/cbmr.1996.0014.

Craddock, R.C., James, G.A., Holtzheimer, P.E., Hu, X.P.P., Mayberg, H.S., 2012. A whole brain fMRI atlas generated via spatially constrained spectral clustering. Hum. Brain Mapp. 33, 1914–1928. doi:10.1002/hbm.21333.

Craig, A.D., 2002. How do you feel? Interoception: the sense of the physiological condition of the body. Nat. Rev. Neurosci. 3, 655–666. doi:10.1038/nrn894.

D'Souza, D.V., Jonckers, E., Bruns, A., Kunnecke, B., von Kienlin, M., Van der Linden, A., Mueggler, T., Verhoye, M., 2014. Preserved modular network organization in the sedated rat brain. PLoS One 9. doi:10.1371/journal.pone.0106156.

De Vico Fallani, F., Richiardi, J., Chavez, M., Achard, S., 2014. Graph analysis of functional brain networks: practical issues in translational neuroscience. Philosop. Trans. R. Soc. Lond. 369, 1653. doi:10.1098/rstb.2013.0521.

Deacon, T.W., 1990. Rethinking mammalian brain evolution. Am. Zool. 30, 629–705.

Dixon, M.L., De la Vega, A., Mills, C., Andrews-Hanna, J., Spreng, R.N., Cole, M.W., Christoff, K., 2018. Heterogeneity within the frontoparietal control network and its relationship to the default and dorsal attention networks. Proc. Natl. Acad. Sci. USA 115, E1598–E1607. doi:10.1073/pnas.1715766115.

Ezran, C., Karanewsky, C.J., Pendleton, J.L., Sholtz, A., Krasnow, M.R., Willick, J., Razafindrakoto, A., Zohdy, S., Albertelli, M.A., Krasnow, M.A., 2017. The mouse lemur, a genetic model organism for primate biology, behavior, and health. Genetics 206, 651–664. doi:10.1534/genetics.116.199448.

Farrant, K., Uddin, L.Q., 2015. Asymmetric development of dorsal and ventral attention networks in the human brain. Dev. Cogn. Neurosci. 12, 165–174. doi:10.1016/j.dcn.2015.02.001.

Fattori, P., Breveglieri, R., Bosco, A., Gamberini, M., Galletti, C., 2017. Vision for prehension in the medial parietal cortex. Cereb. Cortex 27, 1149–1163. doi:10.1093/cercor/bhv302.

Friston, K.J., Holmes, A.P., Worsley, K.J., Poline, J.P., Frith, C.D., Frackowiak, R.S.J., 1994. Statistical parametric maps in functional imaging: a general linear approach. Hum. Brain Mapp. 2, 189–210. doi:10.1002/hbm.460020402.

Ghahremani, M., Hutchison, R.M., Menon, R.S., Everling, S., 2017. Frontoparietal functional connectivity in the common marmoset. Cereb. Cortex 27, 3890–3905. doi:10.1093/cercor/bhw198.

Glasser, M.F., Coalson, T.S., Robinson, E.C., Hacker, C.D., Harwell, J., Yacoub, E., Ugurbil, K., Andersson, J., Beckmann, C.F., Jenkinson, M., Smith, S.M., Van Essen, D.C., 2016. A multi-modal parcellation of human cerebral cortex. Nature 536, 171–178. doi:10.1038/nature18933.

Gorgolewski, K., Burns, C.D., Madison, C., Clark, D., Halchenko, Y.O., Waskom, M.L., Ghosh, S.S., 2011. Nipype: a flexible, lightweight and extensible neuroimaging

data processing framework in python. Front. Neuroinform. 5. doi:10.3389/fninf.2011.00013.
Goulden, N., Khusnulina, A., Davis, N.J., Bracewell, R.M., Bokde, A.L., McNulty, J.P., Mullins, P.G., 2014. The salience network is responsible for switching between the default mode network and the central executive network: replication from DCM. Neuroimage 99, 180–190. doi:10.1016/j.neuroimage.2014.05.052.
Grandjean, J., Zerbi, V., Balsters, J.H., Wenderoth, N., Rudin, M., 2017. Structural basis of large-scale functional connectivity in the mouse. J. Neurosci. 37, 8092–8101. doi:10.1523/JNEUROSCI.0438-17.2017.
Greicius, M.D., Kiviniemi, V., Tervonen, O., Vainionpaa, V., Alahuhta, S., Reiss, A.L., Menon, V., 2008. Persistent default-mode network connectivity during light sedation. Hum. Brain Mapp. 29, 839–847. doi:10.1002/hbm.20537.
Hagberg, A.A., Schult, D.A., Swart, P.J., 2008. Exploring network structure, dynamics, and function using NetworkX. In: Proceedings of the 7th Python in Science Conference. Pasadena, CA.
Herculano-Houzel, S., Catania, K., Manger, P.R., Kaas, J.H., 2015. Mammalian brains are made of these: a dataset of the numbers and densities of neuronal and nonneuronal cells in the brain of glires, primates, scandentia, eulipotyphlans, afrotherians and artiodactyls, and their relationship with body mass. Brain Behav. Evolut. 86, 145–163. https://doi.org/10.1159/000437413.
Hopfinger, J.B., Buonocore, M.H., Mangun, G.R., 2000. The neural mechanisms of top-down attentional control. Nat. Neurosci. 3, 284–291 https://doi.org/WOS:000085810500019.
Hori, Y., Schaeffer, D.J., Gilbert, K.M., Hayrynen, L.K., Cléry, J.C., Gati, J.S., Menon, R.S., Everling, S., 2020. Altered resting-state functional connectivity between awake and isoflurane anesthetized marmosets. Cereb. Cortex. 18 June 2020 https://doi.org/10.1093/cercor/bhaa168 .
Hutchison, R.M., Womelsdorf, T., Gati, J.S., Leung, L.S., Menon, R.S., Everling, S., 2012. Resting-state connectivity identifies distinct functional networks in macaque cingulate cortex. Cereb. Cortex 22, 1294–1308. https://doi.org/10.1093/cercor/bhr181.
Jacobs, L.F., Schenk, F., 2003. Unpacking the cognitive map: the parallel map theory of hippocampal function. Psych. Rev. 110, 285–315. doi:10.1037/0033-295X.110.2.285.
Janak, P.H., Tye, K.M., 2015. From circuits to behaviour in the amygdala. Nature 517, 284–292. doi:10.1038/nature14188.
Knudsen, E.I., 2011. Control from below: the role of a midbrain network in spatial attention. Eur. J. Neurosci. 33, 1961–1972. doi:10.1111/j.1460-9568.2011.07696.x.
Lambiotte, R., Delvenne, J.-C., Barahona, M., 2015. Laplacian dynamics and multiscale modular structure in networks. IEEE Trans. Netw. Sci. Eng. 1, 76–90. https://doi.org/10.1109/TNSE.2015.2391998.
Le Gros Clark, W.E., 1931. The brain of *Microcebus murinus*. Proc. Zool. Soc. Lond. 101, 463–486.
Ledoit, O., Wolf, M., 2004. A well-conditioned estimator for large-dimensional covariance matrices. J. Multivar. Anal. 88, 365–411. doi:10.1016/S0047-259x(03)00096-4.
Lee, M.H., Hacker, C.D., Snyder, A.Z., Corbetta, M., Zhang, D., Leuthardt, E.C., Shimony, J.S., 2012. Clustering of resting state networks. PLoS One 7, e40370. doi:10.1371/journal.pone.0040370.
Li, L.C., Hu, X.P., Preuss, T.M., Glasser, M.F., Damen, F.W., Qiu, Y.X., Rilling, J., 2013. Mapping putative hubs in human, chimpanzee and rhesus macaque connectomes via diffusion tractography. Neuroimage 80, 462–474. doi:10.1016/j.neuroimage.2013.04.024.
Liang, Z.F., King, J.A., Zhang, N.Y., 2011. Uncovering intrinsic connectional architecture of functional networks in awake rat brain. J. Neurosci. 31, 3776–3783. doi:10.1523/Jneurosci.4557-10.2011.
Liska, A., Galbusera, A., Schwarz, A.J., Gozzi, A., 2015. Functional connectivity hubs of the mouse brain. Neuroimage 115, 281–291. doi:10.1016/j.neuroimage.2015.04.033.
Liu, C.R., Yen, C.C., Szczupak, D., Ye, F.Q., Leopold, D.A., Silva, A.C., 2019. Anatomical and functional investigation of the marmoset default mode network. Nat. Commun. 10. doi:10.1038/S41467-019-09813-7.
Mantini, D., Gerits, A., Nelissen, K., Durand, J.B., Joly, O., Simone, L., Sawamura, H., Wardak, C., Orban, G.A., Buckner, R.L., Vanduffel, W., 2011. Default mode of brain function in monkeys. J. Neurosci. 31, 12954–12962. doi:10.1523/JNEUROSCI.2318-11.2011.
Mattis, S., 1976. Mental status examination for organic mental syndrome in the elderly patients. In: Bellak, L., Karasu, T. (Eds.), Geriatrics Psychiatry: a Handbook for Psychiatrists and Primary Care Physicians. Grune & Stratton, New York, pp. 77–121.
Mechling, A.E., Hubner, N.S., Lee, H.L., Hennig, J., von Elverfeldt, D., Harsan, L.A., 2014. Fine-grained mapping of mouse brain functional connectivity with resting-state fMRI. Neuroimage 96, 203–215. doi:10.1016/j.neuroimage.2014.03.078.
Mensch, A., Mairal, J., Thirion, B., Varoquaux, G., 2016. Dictionary learning for massive matrix factorization. In: Proceedings of the 33rd International Conference on Machine Learning & Memory. Cold Spring Harbor, N.Y.
Mevel, K., Landeau, B., Fouquet, M., La Joie, R., Villain, N., Mezenge, F., Perrotin, A., Eustache, F., Desgranges, B., Chetelat, G., 2013. Age effect on the default mode network, inner thoughts, and cognitive abilities. Neurobiol. Aging 34, 1292–1301. doi:10.1016/j.neurobiolaging.2012.08.018.
Migliaccio, R., Gallea, C., Kas, A., Perlbarg, V., Samri, D., Trotta, L., Michon, A., Lacomblez, L., Dubois, B., Lehericy, S., Bartolomeo, P., 2016. Functional connectivity of ventral and dorsal visual streams in posterior cortical atrophy. J. Alzheimers Dis. 51, 1119–1130. doi:10.3233/Jad-150934.
Miranda-Dominguez, O., Mills, B.D., Grayson, D., Woodall, A., Grant, K.A., Kroenke, C.D., Fair, D.A., 2014. Bridging the gap between the Human and Macaque connectome: A quantitative comparison of global interspecies structure-function relationships and network topology. J. Neurosci. 34, 5552–5563. doi:10.1523/Jneurosci.4229-13.2014.
Mota, B., Herculano-Houzel, S., 2015. Cortical folding scales universally with surface area and thickness, not number of neurons. Science 349, 74–77. doi:10.1126/science.aaa9101.
Mutlu, J., Landeau, B., Gaubert, M., de La Sayette, V., Desgranges, B., Chetelat, G., 2017. Distinct influence of specific versus global connectivity on the different Alzheimer's disease biomarkers. Brain 140, 3317–3328. doi:10.1093/brain/awx279.
Nadkarni, N.A., Bougacha, S., Garin, C., Dhenain, M., Picq, J.L., 2019. A 3D population-based brain atlas of the mouse lemur primate with examples of applications in aging studies and comparative anatomy. Neuroimage 185, 85–95. doi:10.1016/j.neuroimage.2018.10.010.
Newman, M.E.J., 2006. Modularity and community structure in networks. Proc. Natl. Acad. Sci. USA 103, 8577–8582. doi:10.1073/pnas.0601602103.
Oguz, I., Zhang, H., Rumple, A., Sonka, M., 2014. RATS: rapid automatic tissue segmentation in rodent brain MRI. J. Neurosci. Methods 221, 175–182. doi:10.1016/j.jneumeth.2013.09.021.
Paasonen, J., Stenroos, P., Salo, R.A., Kiviniemi, V., Grohn, O., 2018. Functional connectivity under six anesthesia protocols and the awake condition in rat brain. Neuroimage 172, 9–20. doi:10.1016/j.neuroimage.2018.01.014.
Power, J.D., Mitra, A., Laumann, T.O., Snyder, A.Z., Schlaggar, B.L., Petersen, S.E., 2014. Methods to detect, characterize, and remove motion artifact in resting state fMRI. Neuroimage 84, 320–341. doi:10.1016/j.neuroimage.2013.08.048.
Raichle, M.E., 2011. The restless brain. Brain Connect. 1, 3–12. doi:10.1089/brain.2011.0019.
Rolls, E.T., 2019. The cingulate cortex and limbic systems for emotion, action, and memory. Brain Struct. Funct. 224, 3001–3018. doi:10.1007/s00429-019-01945-2.
Rolls, E.T., Joliot, M., Tzourio-Mazoyer, N., 2015. Implementation of a new parcellation of the orbitofrontal cortex in the automated anatomical labeling atlas. Neuroimage 122, 1–5. doi:10.1016/j.neuroimage.2015.07.075.
Sierakowiak, A., Monnot, C., Aski, S.N., Uppman, M., Li, T.Q., Damberg, P., Brene, S., 2015. Default mode network, motor network, dorsal and ventral basal ganglia networks in the rat brain: comparison to human networks using resting state-fMRI. PLoS One 10, e0120345. doi:10.1371/journal.pone.0120345.
Snyder, L.H., Batista, A.P., Andersen, R.A., 1997. Coding of intention in the posterior parietal cortex. Nature 386, 167–170. doi:10.1038/386167a0.
Sole-Padulles, C., Castro-Fornieles, J., de la Serna, E., Calvo, R., Baeza, I., Moya, J., Lazaro, L., Rosa, M., Bargallo, N., Sugranyes, G., 2016. Intrinsic connectivity networks from childhood to late adolescence: effects of age and sex. Dev. Cogn. Neurosc. 17, 35–44. doi:10.1016/j.dcn.2015.11.004.
Telesford, Q.K., Joyce, K.E., Hayasaka, S., Burdette, J.H., Laurienti, P.J., 2011. The ubiquity of small-world networks. Brain Connect. 1, 5. doi:10.1089/brain.2011.0038.
Tzourio-Mazoyer, N., Landeau, B., Papathanassiou, D., Crivello, F., Etard, O., Delcroix, N., Mazoyer, B., Joliot, M., 2002. Automated anatomical labeling of activations in SPM using a macroscopic anatomical parcellation of the MNI MRI single-subject brain. Neuroimage 15, 273–289. doi:10.1006/nimg.2001.0978.
van den Heuvel, M.P., Bullmore, E.T., Sporns, O., 2016. Comparative connectomics. Trends Cogn. Sci. 20, 345–361. doi:10.1016/j.tics.2016.03.001.
van den Heuvel, M.P., Sporns, O., 2013. Network hubs in the human brain. Trends Cogn. Sci. 17, 683–696. doi:10.1016/j.tics.2013.09.012.
Varoquaux, G., Gramfort, A., Poline, J.B., Thirion, B., 2012. Markov models for fMRI correlation structure: is brain functional connectivity small world, or decomposable into networks? J. Physiol. Paris 106, 212–221. doi:10.1016/j.jphysparis.2012.01.001.
Vincent, J.L., Patel, G.H., Fox, M.D., Snyder, A.Z., Baker, J.T., Van Essen, D.C., Zempel, J.M., Snyder, L.H., Corbetta, M., Raichle, M.E., 2007. Intrinsic functional architecture in the anaesthetized monkey brain. Nature 447, 83–86. doi:10.1038/nature05758.
Watts, D.J., Strogatz, S.H., 1998. Collective dynamics of 'small-world' networks. Nature 393, 440–442. doi:10.1038/30918.
Wen, X., Yao, L., Fan, T., Wu, X., Liu, J., 2012. The spatial pattern of basal ganglia network: a resting state fMRI study. In: ICME International Conference on Complex Medical Engineering (CME), pp. 43–46. doi:10.1109/ICCME.2012.6275632.
Wenk, G.L., 1997. The nucleus basalis magnocellularis cholinergic system: one hundred years of progress. Neurobiol. Learn. Mem. 67, 85–95. doi:10.1006/nlme.1996.3757.
Yeo, B.T.T., Krienen, F.M., Sepulcre, J., Sabuncu, M.R., Lashkari, D., Hollinshead, M., Roffman, J.L., Smoller, J.W., Zoller, L., Polimeni, J.R., Fischl, B., Liu, H.S., Buckner, R.L., 2011. The organization of the human cerebral cortex estimated by intrinsic functional connectivity. J. Neurophysiol. 106, 1125–1165. doi:10.1152/jn.00338.2011.
Yushkevich, P.A., Piven, J., Hazlett, H.C., Smith, R.G., Ho, S., Gee, J.C., Gerig, G., 2006. User-guided 3D active contour segmentation of anatomical structures: significantly improved efficiency and reliability. Neuroimage 31, 1116–1128. doi:10.1016/j.neuroimage.2006.01.015.
Zhou, Y., Friston, K.J., Zeidman, P., Chen, J., Li, S., Razi, A., 2018. The hierarchical organization of the default, dorsal attention and salience networks in adolescents and young adults. Cereb. Cortex 28, 726–737. doi:10.1093/cercor/bhx307.
Zilles, K., Rehkamper, G., Schleicher, A., 1979. A quantitative approach to cytoarchitectonics. V. The areal pattern of the cortex of microcebus murinus (E. Geoffroy 1828), (Lemuridae, primates). Anat. Embryol. 157, 269–289. doi:10.1007/BF00304994.